TECHNICAL ARTICLE

Electron-density distribution and disordered crystal structure of 12*H*-SiAlON, $SiAl_5O_2N_5$

Hiroki Banno,[1] Takaaki Hanai,[1] Toru Asaka,[1] Koji Kimoto,[2] Hiromi Nakano,[3] and Koichiro Fukuda[1,a)]
[1]*Department of Materials Science and Engineering, Nagoya Institute of Technology, Nagoya 466-8555, Japan*
[2]*Advanced Key Technologies Division, National Institute for Materials Science, Tsukuba 305-0044, Japan*
[3]*Cooperative Research Facility Center, Toyohashi University of Technology, Toyohashi 441-8580, Japan*

(Received 16 December 2013; accepted 7 March 2014)

The crystal structure of $SiAl_5O_2N_5$ was characterized by laboratory X-ray powder diffraction ($CuK\alpha_1$). The title compound is hexagonal with space group $P6_3/mmc$ ($Z = 2$). The unit-cell dimensions are $a = 0.303153(3)$ nm, $c = 3.28153(3)$ nm, and $V = 0.261178(5)$ nm^3. The initial structural model was successfully derived by the direct methods and further refined by the Rietveld method. The final structural model showed the positional disordering of two of the four (Si,Al) sites. The maximum-entropy method-based pattern fitting (MPF) method was used to confirm the validity of the split-atom model, in which conventional structure bias caused by assuming intensity partitioning was minimized. The reliability indices calculated from the MPF were $R_{wp} = 5.00\%$, S ($=R_{wp}/R_e$) $= 1.25$, $R_p = 3.76\%$, $R_B = 1.26\%$, and $R_F = 0.90\%$. The disordered crystal structure was successfully described by overlapping four types of domains with ordered atom arrangements. The distribution of atomic positions in each of the domains can be achieved in the space group $P6_3mc$. Two of the four types of domains are related by a pseudo-symmetry inversion, and the two remaining domains also have each other the inversion pseudo-symmetry. © *2014 International Centre for Diffraction Data.*
[doi:10.1017/S0885715614000396]

Key words: 12*H*-SiAlON, X-ray powder diffraction, Rietveld method, maximum-entropy method, electron-density distributions, crystal structures

I. INTRODUCTION

Silicon aluminium oxynitride (SiAlON) compounds are technically important materials for high-temperature engineering applications. In the quaternary system Si_3N_4–SiO_2–Al_2O_3–AlN, there are six SiAlON polytypoids (8*H*, 15*R*, 12*H*, 21*R*, 27*R*, and 2*H*) established so far at the compositions between β-SiAlON and AlN (Jack, 1976). In the notation of Ramsdell (Parthé, 1964), the polytypoids with the general formula $(Si,Al)_m(O,N)_{m+1}$ are denoted as $2mH$ (m even) and $3mR$ (m odd). Banno *et al.* (2014) have characterized the crystal structure of 15*R*-SiAlON ($SiAl_4O_2N_4$) by X-ray powder diffraction method (XRPD). The crystal structure has been expressed by a split-atom model ($a = 0.301332(3)$ nm, $c = 4.18616(4)$ nm, and space group $R\bar{3}m$) showing the positional disordering of one of the three (Si,Al) sites. This disordered structure has been interpreted to be a statistical average of the three types of domains with ordered structures. Bando *et al.* (1986) have investigated the crystal structure as well as chemical composition of 12*H*-SiAlON ($SiAl_5O_2N_5$) using the high-resolution transmission electron microscope (TEM) equipped with energy dispersive X-ray spectrometer and electron energy loss spectrometer. The convergent beam electron diffraction (CBED) patterns showed the possible space groups to be $P6_3mc$ and $P6_3/mmc$. Since the mirror plane normal to the *c*-axis was absent for the structure image that was obtained from the square area of about 6.3 nm each side, they proposed the disordered structural model with the space group $P6_3mc$. Their structural model is characterized by the splitting of two of the six independent (Si,Al) sites in the unit cell.

For aluminium oxynitride (AlON) polytypoids with the general formula $Al_nO_3N_{n-2}$ (Sakai, 1978; Bartram and Slack, 1979; Tabary and Servant, 1998, 1999a, 1999b), the crystal structures of 21*R* ($n = 7$) (Asaka *et al.*, 2013a) and 27*R* ($n = 9$) (Asaka *et al.*, 2013b) have been successfully determined using the recent analytical techniques for XRPD data as described below. The crystal structures have shown positional disordering of two of the four types of Al sites for 21*R* and two of the five types of Al sites for 27*R*. Each disordered structure with the space group $R\bar{3}m$ has been considered to be a statistical average of five types of the structural configurations with ordered atom arrangements. The distribution of atomic positions in one of the structural configurations can be achieved in the space group $R\bar{3}m$ (centrosymmetric). The atom arrangements in the four other configurations are noncentrosymmetric with the space group $R3m$.

Recent advances in the field of crystal-structure analysis from XRPD data have enabled us to investigate unknown structures as well as complex structures, including positional disordering of atoms. To begin with initial structural models are required, which may be determined by, for example, direct methods (Giacovazzo, 1992). The structural parameters are subsequently refined using the Rietveld method (Rietveld, 1967). A combined use of the Rietveld method, the maximum-entropy method (MEM) (Takata *et al.*, 2001), and

a)Author to whom correspondence should be addressed. Electronic mail: fukuda.koichiro@nitech.ac.jp

the MEM-based pattern fitting (MPF) method (Izumi, 2004) has enabled us to disclose new structural details. MEM is capable of estimating structure factors of unobserved reflections and improving those of overlapped reflections, which give MEM advantages over the classical Fourier method. However, the Rietveld method and MEM have a drawback in determining the electron-density distributions (EDDs) because the observed structure factors, F_o(Rietveld), are biased towards the structural model assuming intensity partitioning. On the other hand, the MPF method can minimize the structural bias. Thus, MEM analyses and whole-pattern fitting are alternately repeated (REMEDY cycles) until a reliability index, R_{wp}, reaches a minimum (Izumi *et al.*, 2001). Crystal structures can be seen clearly from EDDs determined by MPF.

In the present study, we have prepared a sintered specimen of 12*H*-SiAlON, $SiAl_5O_2N_5$. We determined the initial structural model from XRPD data using direct methods and further modified it into the split-atom model. The validity of the structural model was confirmed by the three-dimensional (3D) EDDs determined by the MPF method.

II. EXPERIMENTAL

A. Material

The reagent-grade chemicals of Si_3N_4 (99.9%, KCL Co., Ltd., Saitama, Japan), Al_2O_3 (99%, Taimei Chemicals Co. Ltd., Nagano, Japan), and AlN (99.9%, KCL Co., Ltd., Saitama, Japan) were mixed in molar ratios of (Si_3N_4:Al_2O_3:AlN) = (1:2:11), corresponding to (Si:Al:O:N) = (1:5:2:5). The well-mixed chemicals were heated under a nitrogen pressure of 0.1 MPa at 2023 K for 1 h, followed by cooling to ambient temperature by cutting furnace power. The reaction product was a slightly sintered polycrystalline material consisting mainly of $SiAl_5O_2N_5$ with a small amount of 15*R*-SiAlON ($SiAl_4O_2N_4$).

B. Characterization

A part of the sintered material was finely ground to obtain powder specimen and introduced into a glass capillary tube of internal diameter approximately 0.4 mm. The XRPD intensities were collected on a diffractometer in the Debye–Scherrer geometry (SmartLab, Rigaku Co., Tokyo, Japan), which was equipped with an incident-beam Ge(111) Johansson monochromator to obtain Cu$K\alpha_1$ radiation and a high-speed detector (Rigaku D/teX). The X-ray generator was operated at 45 kV and 200 mA. Other experimental conditions were: continuous scan, experimental 2θ range from 3.0° to 158.0° and a scan speed 0.2°/min, 15 501 total data points, and 12.9 h total experimental time. No preferred orientation could be seen in the diffraction pattern which was collected with the specimen rotating. We corrected the X-ray absorption using the μr value (where μ is the linear absorption coefficient and r is the sample radius) of the sample and capillary tube, which was determined by the transmittance of direct incident beam. The structure data were standardized according to rules formulated by Parthé and Gelato (1984) using the computer program STRUCTURE TIDY (Gelato and Parthé, 1987). The crystal-structure models, equidensity isosurfaces of EDDs, and two-dimensional EDD map were visualized with the computer program VESTA (Momma and Izumi, 2011).

III. RESULTS AND DISCUSSION

A. Crystal-structure determination and refinement

The XRPD pattern in Figure 1 showed the presence of weak diffraction intensities peculiar to 15*R*-SiAlON ($SiAl_4O_2N_4$). All of the other diffraction peaks were successfully indexed with a hexagonal unit cell of $a \approx 0.303$ nm and $c \approx 3.28$ nm. The observed diffraction peaks were examined to confirm the presence or absence of reflections. Systematic absences $l \neq 2n$ for $hh\bar{2}hl$ reflections were found, which implies that possible space groups are $P6_3mc$, $P\bar{6}2c$, and $P6_3/mmc$. All of the possible space groups were tested using the EXPO2009 package (Altomare *et al.*, 2009) for crystal-structure determination. The individual integrated intensities, which were refined by the Le Bail method (Le Bail *et al.*, 1988) embedded on the computer program RIETAN-FP, were used for the direct methods. Because the atomic

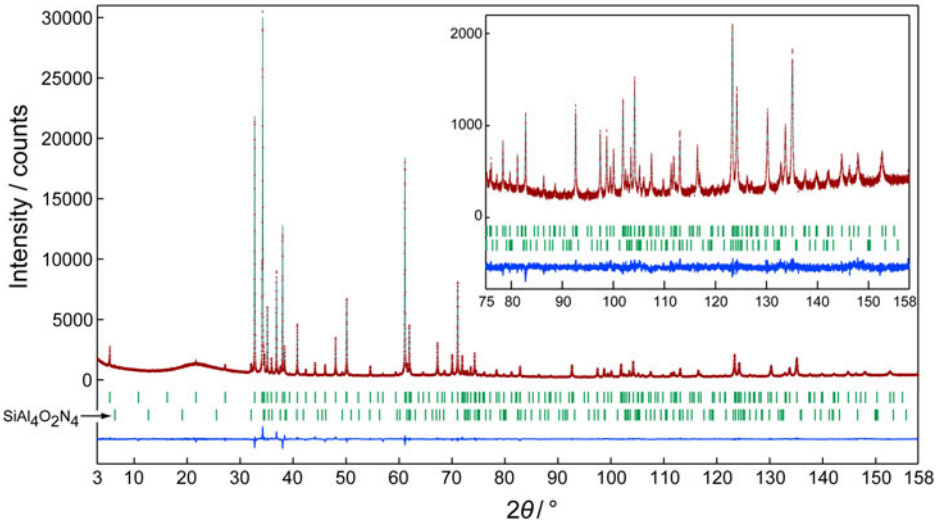

Figure 1. (Color online) Comparison of the observed diffraction patterns of 12*H*-SiAlON ($SiAl_5O_2N_5$) and 15*R*-SiAlON ($SiAl_4O_2N_4$) (symbol: +) with the corresponding calculated pattern (upper solid line). The difference curve is shown in the lower part of the diagram. Vertical bars indicate the positions of possible Bragg reflections.

https://doi.org/10.1017/S0885715614000396 Published online by Cambridge University Press

scattering factors of Si and Al and those of O and N are nearly the same, a unit-cell content of [12Al 14N] was used as input data for the search of an initial structural model. A promising structural model with the minimum reliability index R_F (Young, 1993) of 22.3% was successfully obtained for the space group $P6_3/mmc$. There are eight independent sites in the unit cell; four (Si,Al) sites at Wyckoff positions 2*a* ((Si, Al)1), 4*e* ((Si,Al)2), 4*f* ((Si,Al)3), and 2*c* ((Si,Al)4), and four (O,N) sites at 2*b* ((O,N)1), 4*e* ((O,N)2) and 4*f* ((O,N)3 and (O,N)4).

The structural parameters of all atoms were subsequently refined by the Rietveld method using the computer program RIETAN-FP (Izumi and Momma, 2007). The structural model of 15*R*-SiAlON ($SiAl_4O_2N_4$) (Banno *et al.*, 2014) was included in the refinement as the coexisting phase. A Legendre polynomial was fitted to background intensities with 12 adjustable parameters. The split pseudo-Voigt function (Toraya, 1990) was used to fit the peak profile. The Si and Al atoms as well as the O and N atoms were assumed to be randomly distributed over the same sites in the crystal structure, although there might be the site preference of these atoms; the site occupancy factors (sof) of Si and Al atoms in each (Si,Al) site were fixed at sof(Si) = 1/6 and sof (Al) = 5/6 and those of O and N atoms in each (O,N) site were fixed at sof(O) = 2/7 and sof(N) = 5/7. The isotropic displacement (U) parameters for (O,N) sites were constrained to be equal. The refinement, however, resulted in the relatively large U parameters for the (Si,Al)2 and (Si,Al)4 sites (U((Si, Al)2) = 2.60(4) × 10^{-2} nm^2 and U((Si,Al)4) = 5.39(7) × 10^{-2} nm^2) with the less satisfactory reliability (R) indices (Young, 1993) of R_{wp} = 10.03%, S (=R_{wp}/R_e) = 2.51, R_p = 7.13%, R_B = 8.29%, and R_F = 5.98%. These findings promoted us to build split-atom model for these sites.

In the split-atom model, the (Si,Al)2 site was split into two independent crystallographic sites of (Si,Al)2A and (Si, Al)2B with the same Wyckoff position 4*e*. The distribution of (Si,Al) atoms between each of these sites was determined by imposing the linear constraint of sof((Si,Al)2A) + sof((Si, Al)2B) = 1. The parameters U((Si,Al)2A) and U((Si,Al)2B) were constrained to be equal. Because the sof values and corresponding U parameters were strongly correlated, they were refined alternately in successive least-squares cycles. With the (Si,Al)4 site, the site symmetry was decreased from 2*c* (point symmetry $\bar{6}m2$) to 4*f* (3*m*). The subsequent Rietveld refinement resulted in satisfactory U parameters for all the sites with R indices of R_{wp} = 5.43%, S = 1.36, R_p = 4.23%, R_B = 4.62% and R_F = 3.00%, indicating that the disordered arrangements of (Si,Al)2 and (Si,Al)4 sites can be represented adequately with the split-atom model in Figure 2. The separation distances of atoms are 0.0725(4) nm for (Si,Al)2A–(Si,Al)2B and 0.0834(3) nm for the split (Si,Al)4 site. Crystal data are given in Table I, and the final atomic positional and U parameters are given in Table II. It should be noted that the sof values of (Si,Al)2A and (Si,Al)2B are, respectively, nearly equal to 3/4 and 1/4. Selected interatomic distances, together with their standard deviations, are listed in Table III.

Quantitative X-ray analysis procedure was implemented in the program RIETAN-FP. The phase composition of the sample was found to be 94.2 mol% 12*H*-SiAlON ($SiAl_5O_2N_5$) and 5.8 mol% 15*R*-SiAlON ($SiAl_4O_2N_4$). The average chemical composition corresponds to the atom ratios

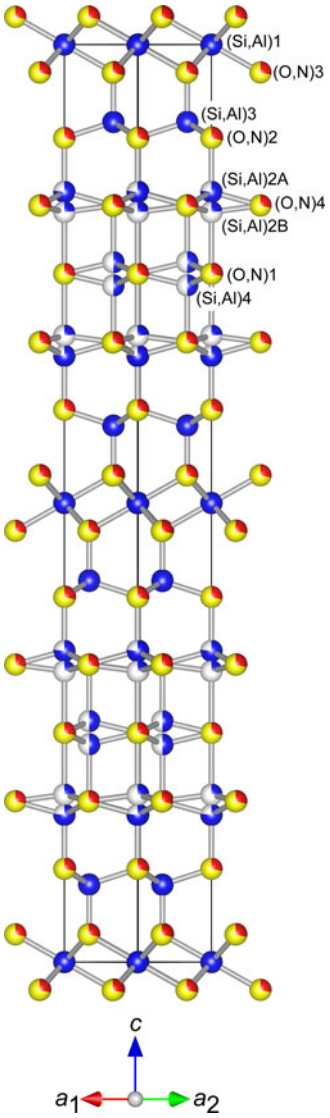

Figure 2. (Color online) Crystal structure of $SiAl_5O_2N_5$. All the atoms are expressed as solid spheres. Because the occupancies of (Si,Al)2A, (Si,Al) 2B, and (Si,Al)4 sites are less than unity, the (Si,Al) atoms occupying there are displayed as blue circle graphs for occupancies. Red and yellow bicolour balls are for oxygen (red) and nitrogen (yellow) sites. Atom numbering corresponds to that given in Table II.

of (Si:Al:O:N) = (1:4.942:2:4.942). Thus, the secondary phase was probably produced by the error in weighing of the reagents; the amount of AlN was relatively smaller than those of Si_3N_4 and Al_2O_3. The AlN readily reacts with water in air to form $Al(OH)_3$ and NH_3, which would mainly cause the weighing error for AlN.

The MPF method was subsequently used to confirm the validity of the split-atom model. The EDDs with 30 × 30 ×

TABLE I. Crystal data for $SiAl_5O_2N_5$.

Chemical composition	$SiAl_5O_2N_5$
Space group	$P6_3/mmc$
a (nm)	0.303153(3)
c (nm)	3.28153(3)
V (nm^3)	0.261178(5)
Z	2
D_x (Mg m^{-3})	3.370

https://doi.org/10.1017/S0885715614000396 Published online by Cambridge University Press

TABLE II. Structural parameters for $SiAl_5O_2N_5$[a].

Site	Wyckoff position	sof	x	y	z	$10^4 \times U$ (nm^2)
(Si,Al)1	2*a*	1	0	0	0	1.84(3)
(Si,Al)2A	4*e*	0.767(2)	0	0	0.16057(5)	0.69(3)
(Si,Al)2B	4*e*	0.233	0	0	0.18266(15)	0.69
(Si,Al)3	4*f*	1	1/3	2/3	0.08441(3)	0.89(2)
(Si,Al)4	4*f*	1/2	1/3	2/3	0.23730(4)	1.07(5)
(O,N)1	2*b*	1	0	0	1/4	1.07(2)
(O,N)2	4*e*	1	0	0	0.10178(5)	1.07
(O,N)3	4*f*	1	1/3	1/3	0.03028(5)	1.07
(O,N)4	4*f*	1	1/3	1/3	0.17546(6)	1.07

[a]Site occupancies: (Si,Al) sites: 16.7% Si and 83.3% Al; (O,N) sites: 28.6% O and 71.4% N.

328 pixels in the unit cell, the spatial resolution of which is approximately 0.010 nm, were obtained from the MPF method using the computer programs RIETAN-FP and Dysnomia (Izumi and Momma, 2011). After two REMEDY cycles, R_B and R_F further decreased to 1.26 and 0.90%, respectively ($R_{wp} = 5.00\%$, $S = 1.25\%$, and $R_p = 3.76\%$). Subtle EDD changes as revealed by MPF significantly improve the R_B and R_F indices. The decrease in R indices demonstrates that the crystal structure can be seen more clearly from EDDs instead of from the conventional structural parameters reported in Table II. Observed, calculated, and difference XRPD patterns for the final MPF are plotted in Figure 1. The EDDs determined by MPF are in reasonably good agreement with the atom arrangements (Figure 3). For example, the 3D EDDs at the (Si,Al)2 and (Si,Al)4 sites were elongated along the *c*-axis, the equidensity isosurfaces of which are in harmony with the atom arrangements. The two-dimensional EDD map at the height of (Si,Al)2 and (Si,Al)4 sites shows that the positions of split (Si,Al) sites are successfully disclosed by the EDDs (Figure 4). We found the peak positions of EDDs from the 3D pixel data and compared them with the coordinates of all atoms that were determined by the Rietveld method. The positional deviations of all atoms in the unit cell were found to be necessarily less than 0.007 nm, which is within the resolution limit of the 3D EDDs. We therefore concluded that, as long as the crystal structure was expressed by a ball-and-stick model, the present split-atom model would be satisfactory.

The structural model determined above is distinct from that proposed by Bando *et al.* (1986). They reported the disordered structural model (space group $P6_3mc$) demonstrating the split (Si,Al) sites, which correspond to the (Si,Al)2 and (Si,Al)3 sites of the present split-atom model.

B. Structure description

The coordination elements of the structure are one [(Si,Al)$(O,N)_6$] octahedron and four types of [(Si,Al)$(O,N)_4$] tetrahedra. The ionic radius of Si^{4+} and Al^{3+} in the six-fold coordination [$r(Si^{4+}(6)) = 0.0400$ nm, $r(Al^{3+}(6)) = 0.0535$ nm, $r(O^{2-}(4)) = 0.138$ nm, and $r(N^{3-}(4)) = 0.146$ nm] (Shannon, 1976) predicts the interatomic distances of 0.178 nm for Si–O, 0.186 nm for Si–N, 0.192 nm for Al–O, and 0.200 nm for Al–N. Thus, the (Si,Al)–(O,N) distance in [(Si,Al)(O,N)]$_6$ octahedron (=0.2013 nm in Table III) is comparable with the Al–O and Al–N distances. The tetrahedrally coordinated Si and Al normally have the interatomic distances of 0.162 nm for Si–O, 0.175 nm for Si–N, 0.175 for Al–O, and 0.187 nm for Al–N (Jack, 1976). Thus, the average interatomic distances of [(Si,Al)$(O,N)_4$] tetrahedra in $SiAl_5O_2N_5$, ranging from 0.183 to 0.188 nm (Table III), indicate that the (O,N) sites would be actually occupied by both O and N

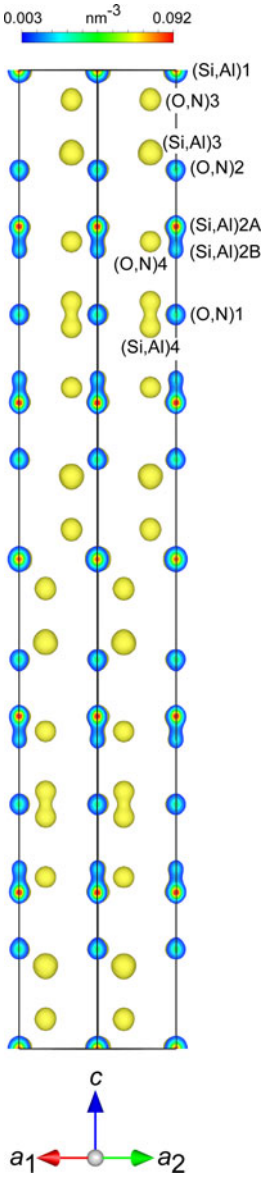

Figure 3. (Color online) Three-dimensional electron-density distributions determined by MPF with the structural model. Isosurfaces expressed in smooth shading style for an equidensity level of 0.003 nm^{-3}.

https://doi.org/10.1017/S0885715614000396 Published online by Cambridge University Press

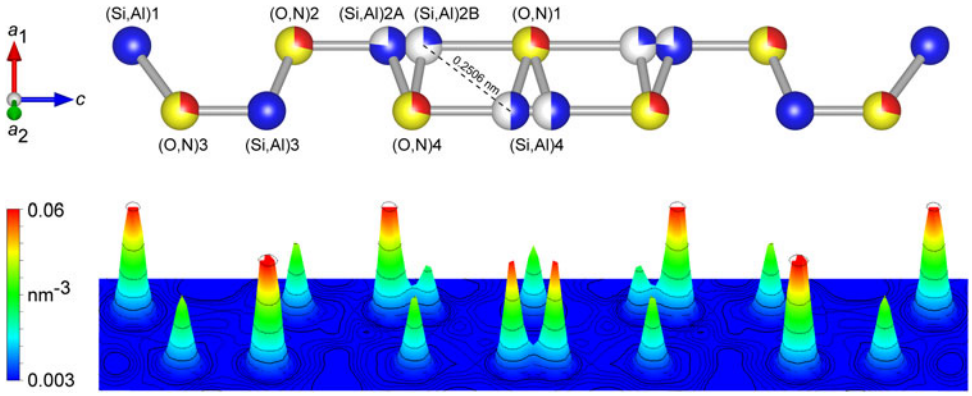

Figure 4. (Color online) A bird's eye view of electron densities up to 42.6% of the maximum (0.141 nm^{-3}) on the plane parallel to (110) (lower part) with the corresponding atomic arrangements (upper part). Because the occupancies of (Si,Al)2A, (Si,Al)2B, and (Si,Al)4 sites are less than unity, the (Si,Al) atoms occupying there are displayed as blue circle graphs for occupancies. Red and yellow bicolour balls are for oxygen (red) and nitrogen (yellow) sites. Atom numbering corresponds to that given in Table II.

TABLE III. Interatomic distances (nm) in $SiAl_5O_2N_5$.

(Si,Al)1–(O,N)3	0.20127(8) × 6
(Si,Al)2A–(O,N)4	0.18172(7) × 3
(Si,Al)2A–(O,N)2	0.1929(2)
<(Si,Al)2A–(O,N)>	0.1845
(Si,Al)2B–(O,N)4	0.17661(7) × 3
(Si,Al)2B–(O,N)1	0.2210(5)
<(Si,Al)2B–(O,N)>	0.1877
(Si,Al)3–(O,N)3	0.1776(2)
(Si,Al)3–(O,N)2	0.18407(6) × 3
<(Si,Al)3–(O,N)>	0.1825
(Si,Al)4–(O,N)4	0.17992(3) × 3
(Si,Al)4–(O,N)4	0.2029(2)
<(Si,Al)4–(O,N)>	0.1857

atoms. There is a possibility of site preference of O and N in the (O,N) sites. However, the information available at present on atom distances is insufficient for the significant results.

In our previous studies on the layered oxycarbides (Iwata *et al.*, 2009; Kaga *et al.*, 2010a, 2010b), oxycarbonitrides (Inuzuka *et al.*, 2010; Urushihara *et al.*, 2011), AlON (Asaka *et al.*, 2013a, 2013b), and 15*R*-SiAlON (Banno *et al.*, 2014), these compounds have been found to be made up of several domains, which are related by pseudo-symmetry inversion. One of the most plausible explanations to interpret the disordered crystal structure of $SiAl_5O_2N_5$ is to, in a similar manner, consider the structure to be a statistical average of several structural configurations. We have successfully extracted four types of *ordered* atom arrangements, which

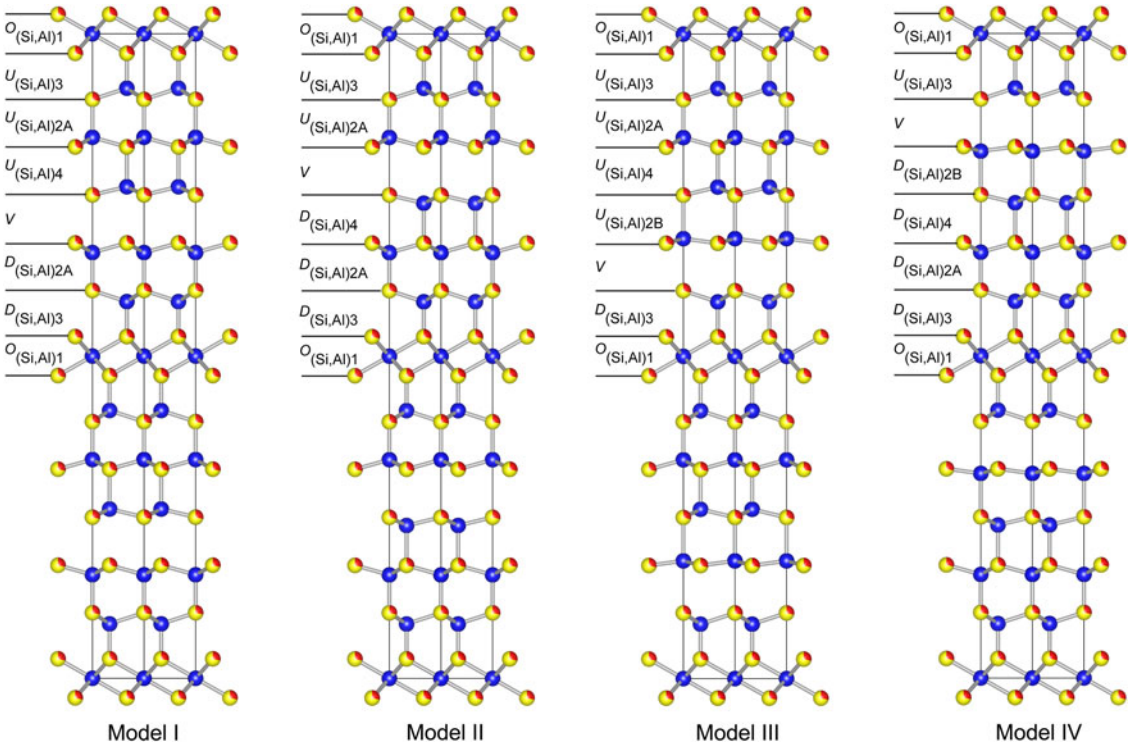

Figure 5. (Color online) Four types of ordered atom arrangements viewed along [110]. Atomic configurational models with the space group $P6_3mc$. The two structural configurations I and II, and those of III and IV are related by the pseudo-symmetry inversion.

https://doi.org/10.1017/S0885715614000396 Published online by Cambridge University Press

TABLE IV. Details of ordered atom-arrangement models.

Model (m)	Number of cation in unit cell (N)					Stacking sequence	Abundance (A)
	(Si,Al)1	(Si,Al)2A	(Si,Al)2B	(Si,Al)3	(Si,Al)4		
I	2	4	0	4	2	$O_{(Si,Al)1}U_{(Si,Al)3}U_{(Si,Al)2A}U_{(Si,Al)4}VD_{(Si,Al)2A}D_{(Si,Al)3}O_{(Si,Al)1}$	1/4
II	2	4	0	4	2	$O_{(Si,Al)1}U_{(Si,Al)3}U_{(Si,Al)2A}VD_{(Si,Al)4}D_{(Si,Al)2A}D_{(Si,Al)3}O_{(Si,Al)1}$	1/4
III	2	2	2	4	2	$O_{(Si,Al)1}U_{(Si,Al)3}U_{(Si,Al)2A}U_{(Si,Al)4}U_{(Si,Al)2B}VD_{(Si,Al)3}O_{(Si,Al)1}$	1/4
IV	2	2	2	4	2	$O_{(Si,Al)1}U_{(Si,Al)3}VD_{(Si,Al)2B}D_{(Si,Al)4}D_{(Si,Al)2A}D_{(Si,Al)3}O_{(Si,Al)1}$	1/4

are termed I–IV (Figure 5), from the parent *disordered* structural model (Figure 2). Since the interatomic distance of 0.2506 nm for (Si,Al)2B–(Si,Al)4 in Figure 4 is unusually short as compared with those of 0.3067 nm for (Si,Al)2A–(Si,Al)4 and 0.3156 nm for (Si,Al)2B–(Si,Al)4, all of the *ordered* models are free from the former atom pairs. Each atom arrangement in the unit cell of the models I–IV is non-centrosymmetric with the space group $P6_3mc$. When the centre of symmetry is removed from the space group $P6_3/mmc$, the resulting space group is $P6_3mc$. The two structural configurations of I and II, and those of III and IV (Figure 5) are therefore related by the pseudo-symmetry inversion. For example with model I, the number of each (Si,Al) atom in the unit cell (N) is $N((Si,Al)1) = 2$, $N((Si,Al)2A) = 4$, $N((Si,Al)3) = 4$, and $N((Si,Al)4) = 2$ (Table IV). This model is characterized by the absence of (Si,Al)2B site. The number of each (Si,Al) atom in the unit cell of the ordered models is summarized in Table IV.

The four types of atom arrangements as mentioned above are made up from three types of basic building elements: (i) the sheet of $[(Si,Al)1(O,N)_6]$ octahedra (the octahedral sheet), (ii) the sheets of $[M(O,N)_4]$ tetrahedra (the tetrahedral sheet), where M = (Si,Al)2A, (Si,Al)2B, (Si,Al)3, and (Si,Al)4, and (iii) the vacant cation sheet, in which the available tetrahedral positions for (Si,Al) atoms are necessarily vacant. The octahedral sheet, denoted by $O_{(Si,Al)1}$, is made up of an array of edge sharing octahedra with (O,N)3 atoms at the corners. In the tetrahedral sheet each $[M(O,N)_4]$ tetrahedron shares three corners, forming a continuous sheet. The unbonded tetrahedral apices of the tetrahedral sheets all point in the same direction; the tetrahedral sheets pointing up along [001] are denoted by U_M, and those pointing down are denoted by D_M. The vacant cation sheet, which is practically composed of two oxygen layers, is denoted by V. For example with model I, the sheet stacking sequence along the c-axis between the two $O_{(Si,Al)1}$ sheets is $\langle O_{(Si,Al)1}U_{(Si,Al)3}U_{(Si,Al)2A}U_{(Si,Al)4}VD_{(Si,Al)2A}D_{(Si,Al)3}O_{(Si,Al)1}\rangle$ (Figure 5). The stacking sequences of the three other models are given in Table IV.

We speculate that the $SiAl_5O_2N_5$ compound with the *disordered* crystal structure is made up of the four types of domains with the *ordered* models (Figure 5 and Table IV). Because the sof values of the disordered structural model are characterized by sof((Si,Al)2A) = 3/4 and sof((Si,Al)2B) = 1/4, we can estimate the abundance (A) of each domain within the $SiAl_5O_2N_5$ compound. The number of cations M in the unit cell of each domain d_m (m = I, II, III, and IV) are summarized in Table IV. Thus, the total number of cations M in the unit cell of the disordered structural model is given by $\Sigma\{A(d_m) \times N(M)_m\}$, where $N(M)_m$ is the number of cations M in the unit cell of the ordered model m. The most simple and plausible $A(d_m)$-values ($\Sigma A(d_m) = 1$) which satisfy the equation of $[\Sigma\{A(d_m) \times N((Si,Al)2A)_m\}:\Sigma\{A(d_m) \times N((Si,Al)2B)_m\}] = [3/4:1/4]$ are $A(d_I) = A(d_{II}) = A(d_{III}) = A(d_{IV}) = 1/4$. This implies that the formation rates of the four domains are exactly the same.

The four types of domains, with the size distribution probably ranging from the unit-cell size to the coherence range of X-rays, would be combined randomly so as to form the whole disordered structure. In the resultant structure, there are vacant sites between the two oxygen layers, which correspond to the vacant cation sheet of the ordered models. When we obtain the CBED patterns under TEM from the relatively wide area where the four types of domains coexist with almost the same abundance of $[A(d_I):A(d_{II}):A(d_{III}):A(d_{IV})] \approx [1:1:1:1]$, they would show the pattern symmetry consistent with the space group $P6_3/mmc$. On the other hand, when we obtain the structure image corresponding to the relatively narrow area where the domain abundance does not meet the above condition, the image can be free from the mirror plane normal to the c-axis. The present domain structure could be formed during crystal growth or high–low phase transformation during cooling. The equal abundance among the four types of domains would be closely related to the formation mechanism of the disordered structure, which should be examined in more detail for the complete clarification.

IV. CONCLUSION

We have clarified the disordered crystal structure of 12*H*-SiAlON ($SiAl_5O_2N_5$), which was satisfactorily represented by the split-atom model with the space group $P6_3/mmc$. The validity of the structural model was confirmed by the EDDs determined by MPF. The disordered crystal structure was interpreted to be a statistical average of the four types of ordered atom arrangements. Each of them was non-centrosymmetric with the space group $P6_3mc$. Two of the four types of domains were related by a pseudo-symmetry inversion, and the two remaining domains also had each other the inversion pseudo-symmetry.

ACKNOWLEDGEMENT

We thank Drs. T. Iwata and H. Toraya, Rigaku Co. Japan, for their technical assistance in XRPD.

Altomare, A., Camalli, M., Cuocci, C., Giacovazzo, C., Moliterni, A. G. G., and Rizzi, R. (**2009**). "EXPO2009: structure solution by powder data in direct and reciprocal space," J. Appl. Crystallogr. **42**, 1197–1202.

Asaka, T., Kudo, T., Banno, H., Funahashi, S., Hirosaki, N., and Fukuda, K. (**2013a**). "Electron density distribution and crystal structure of 21*R*-AlON, $Al_7O_3N_5$," Powder Diffr. **28**, 171–177.

Asaka, T., Banno, H., Funahashi, S., Hirosaki, N., and Fukuda, K. (**2013b**). "Electron density distribution and crystal structure of 27*R*-AlON, $Al_9O_3N_7$," J. Solid State Chem. **204**, 21–26.

Bando, Y., Mitomo, M., Kitami, Y., and Izumi, F. (**1986**). "Structural and composition analysis of silicon aluminium oxynitride polytypes by combined use of structure imaging and microanalysis," J. Microsc. **142**, 235–246.

Banno, H., Hanai, T., Asaka, T., Kimoto, K., and Fukuda, K. (**2014**). "Electron density distribution and disordered crystal structure of 15*R*-SiAlON, $SiAl_4O_2N_4$," J. Solid State Chem. **211**, 124–129.

Bartram, S. F. and Slack, G. A. (**1979**). "$Al_{10}N_8O_3$ and $Al_9N_7O_3$, two new repeated-layer structures in the AlN–Al_2O_3 system," Acta Crystallogr. **B35**, 2281–2283.

Gelato, L. M. and Parthé, E. (**1987**). "STRUCTURE TIDY – a computer program to standardize crystal structure data," J. Appl. Crystallogr. **20**, 139–143.

Giacovazzo, C. (**1992**). *Direct Phasing in Crystallography: Fundamentals and Applications* (Oxford University Press, Oxford).

Inuzuka, H., Kaga, M., Urushihara, D., Nakano, H., Asaka, T., and Fukuda, K. (**2010**). "Synthesis and structural characterization of a new aluminum oxycarbonitride, $Al_5(O, C, N)_4$," J. Solid State Chem. **183**, 2570–2575.

Iwata, T., Kaga, M., Nakano, H., and Fukuda, K. (**2009**). "First discovery and structural characterization of a new compound in Al–Si–O–C system," J. Solid State Chem. **182**, 2252–2260.

Izumi, F. (**2004**). "Beyond the ability of Rietveld analysis: MEM-based pattern fitting," Solid State Ion. **172**, 1–6.

Izumi, F. and Momma, K. (**2007**). "Three-dimensional visualization in powder diffraction," Solid State Phenom. **130**, 15–20.

Izumi, F. and Momma, K. (**2011**). "Three-dimensional visualization of electron- and nuclear-density distributions in inorganic materials by MEM-based technology," IOP Conf. Ser. Mater. Sci. Eng. **18**, 022001.

Izumi, F., Kumazawa, S., Ikeda, T., Hu, W.-Z., Yamamoto, A., and Oikawa, K. (**2001**). "MEM-based structure-refinement system REMEDY and its applications," Mater. Sci. Forum **378–381**, 59–64.

Jack, K. H. (**1976**). "Sialons and related nitrogen ceramics," J. Mater. Sci. **11**, 1135–1158.

Kaga, M., Iwata, T., Nakano, H., and Fukuda, K. (**2010a**). "Synthesis and structural characterization of Al_4SiC_4-homeotypic aluminum silicon oxycarbide, $[Al_{4.4}Si_{0.6}][O_{1.0}C_{2.0}]C$," J. Solid State Chem. **183**, 636–642.

Kaga, M., Urushihara, D., Iwata, T., Sugiura, K., Nakano, H., and Fukuda, K. (**2010b**). "Synthesis and structural characterization of $Al_4Si_2C_5$-homeotypic aluminum silicon oxycarbide, $(Al_{6-x}Si_x)(O_yC_{5-y})$ ($x \sim 0.8$ and $y \sim 1.6$)," J. Solid State Chem. **183**, 2183–2189.

Le Bail, A., Duroy, H., and Fourquet, J. L. (**1988**). "*Ab Initio* structure determination of $LiSbWO_6$ by X-ray powder diffraction," Mater. Res. Bull. **23**, 447–452.

Momma, K. and Izumi, F. (**2011**). "VESTA 3 for three-dimensional visualization of crystal, volumetric and morphology data," J. Appl. Crystallogr. **44**, 1272–1276.

Parthé, E. (**1964**). *Crystal Chemistry of Tetrahedral Structures* (Gordon and Breach, New York).

Parthé, E. and Gelato, L. M. (**1984**). "The standardization of inorganic crystal-structure data," Acta Crystallogr. **A10**, 169–183.

Rietveld, H. M. (**1967**). "Line profiles of neutron powder-diffraction peaks for structure refinement," Acta Crystallogr. **22**, 151–152.

Sakai, T. (**1978**). "Hot-pressing of the AlN-Al_2O_3 system," J. Ceram. Soc. Jpn (Yogyo-Kyokai-shi) **86**, 125–130.

Shannon, R. D. (**1976**). "Revised effective ionic radii and systematic studies of interatomic distances in halides and chalcogenides," Acta Crystallogr. **A32**, 751–767.

Tabary, P. and Servant, C. (**1998**). "Thermodynamic reassessment of the AlN–Al_2O_3 system," Calphad **22**, 179–201.

Tabary, P. and Servant, C. (**1999a**). "Crystalline and microstructure study of the AlN–Al_2O_3 section in the Al–N–O system. I. Polytypes and γ-AlON spinel phase," J. Appl. Crystallogr. **32**, 241–252.

Tabary, P. and Servant, C. (**1999b**). "Crystalline and microstructure study of the AlN–Al_2O_3 section in the Al–N–O system. II. φ′ - and δ-AlON spinel phases," J. Appl. Crystallogr. **32**, 253–272.

Takata, M., Nishibori, E., and Sakata, M. (**2001**). "Charge density studies utilizing powder diffraction and MEM. Exploring of high Tc superconductors, C60 superconductors and manganites," Z. Kristallogr. **216**, 71–86.

Toraya, H. (**1990**). "Array-type universal profile function for powder pattern fitting," J. Appl. Crystallogr. **23**, 485–491.

Urushihara, D., Kaga, M., Asaka, T., Nakano, H., and Fukuda, K. (**2011**). "Synthesis and structural characterization of $Al_7C_3N_3$-homeotypic aluminum silicon oxycarbonitride, $(Al_{7-x}Si_x)$ $(O_yC_zN_{6-y-z})$ ($x \sim 1.2$, $y \sim 1.0$ and $z \sim 3.5$)," J. Solid State Chem. **184**, 2278–2284.

Young, R. A. (**1993**). "Introduction to the Rietveld method" in *The Rietveld Method*, edited by R. A. Young (Oxford University Press, Oxford), pp. 1–38.